Subwavelength Plasmonic Absorbers for Spectrally Selective Resonant Infrared Detectors

Vikrant J. Gokhale, Paul D. Myers and Mina Rais-Zadeh
Department of Electrical Engineering and Computer Science, University of Michigan, Ann Arbor, MI, 48109, USA
minar@umich.edu

Abstract—This work presents the first resonant infrared (IR) detectors with integrated nanostructured subwavelength plasmonic gratings designed to selectively absorb long wavelength infrared (LWIR) radiation. The resonant detectors are the smallest in size demonstrated so far. The absorbers are optimized for a spectral wavelength of 10.15 μm and experimentally demonstrate an absorbance of 46% with a Full Width at Half Maximum (FWHM) of 1.7 μm. The absorbed thermal energy causes a fast (sub-millisecond) proportional change in the frequency of the resonator. The combination of resonant IR detectors with integrated plasmonic absorbers enables spectrally selective IR detectors. Each detector in the array can be optimized for different wavelengths, thus enabling a multi-spectral array for IR spectroscopy and multispectral thermal imaging.

Keywords—micromechanical resonator, IR detector, plasmonics, metamaterial.

I. Introduction

The use of thin-film micromechanical resonators as uncooled infrared (IR) detectors has seen a lot of interest in recent years, because of the potential for high thermal isolation, high sensitivity, and low-noise performance in a small pixel footprint [1]. The materials used for fabricating these resonators have predominantly been piezoelectric materials, such as quartz [1-3], gallium nitride (GaN) [4-6], and aluminum nitride (AlN) [7]. Piezoelectric actuation can offer higher actuation forces in small devices without DC voltages or submicron actuation gaps, such as those required for capacitive actuation. However, these materials are not efficient absorbers of energy in the IR spectrum. The best way of using these materials for IR detectors is to coat the surface of the structures with a thin-film coating that absorbs the IR energy efficiently. Recent work has used simple absorbers such as silicon nitride [4-6], or specially designed nanocomposite thin-films with extremely high broadband absorption efficiency [8].

The use of narrowband (or spectrally selective) IR absorber coatings can enable thermal detectors to achieve the type of narrowband response normally only possible with photonic detectors or specifically designed quarter-wavelength absorber cavities. Narrowband IR detectors can be used for multi-spectral and hyperspectral imaging, where IR information from multiple spectral bands is combined to give a more meaningful image [9]. In order to absorb IR radiation in a narrow spectrum, whose central wavelength can be chosen during design, and convert it efficiently into heat, we make use of surface plasmon resonance (SPR) in a sub-wavelength metallic grating [10-12].

This work was supported in part by the National Science Foundation under Grant# 1002036 and the Army Research Laboratory under contract # W911NF and prepared through participation in the MAST CTA.

II. Theory and Design

A. Theory

A common configuration for exploiting the resonant absorption offered by SPR is the metal-insulator-metal (MIM) structure. In such a geometry, a metal plate is coated by a continuous layer of dielectric material upon which is deposited an array of metal strips. The bottom metal plate is required to be of a thickness greater than the skin depth so as to suppress transmission from the base of the structure, and the thickness of the metal strips is likewise required to exceed the metal skin depth so as to render the effect of the strip thickness negligible on the optical properties of the structure [11]. The physical mechanism that enables the extraordinary optical absorption offered by SPR may be modeled with a simple Fabry-Perot resonator model [10, 11]:

$$\lambda_r = 2n_{eff}w + \lambda_\phi. \quad (1)$$

Here, λ_r is the resonance wavelength, n_{eff} is the effective index of the guided surface plasmon-polariton (SPP) mode, w is the strip width, and λ_ϕ is a constant parameter based on the phase shift incurred upon reflection from the strip terminations. When light is incident upon the MIM cavity, counter-propagating gap surface plasmons develop in the MIM cavity [13]. The mismatch between the effective impedance of the guided cavity mode and the free-space just beyond the strip terminations induces reflections at the strip terminations, thereby causing a standing wave to form in the MIM cavity. When the electromagnetic resonance condition is satisfied, the light incident upon the structure is coupled into the cavity, resulting in perfect absorption in a narrow range about the resonance wavelength.

B. MIM Simulation and Design

While the Fabry-Perot resonance condition given by Eqn. (1) provides a simple description of the physical mechanism responsible for SPR-assisted absorption, effective practical application of this relation is impeded by the difficulty of calculating the λ_ϕ parameter. While analytical formalisms for approximating λ_ϕ exist [12], these methods are often difficult to implement and do not produce sufficiently accurate results for most practical applications; a more useful approach is to model the MIM structure as an effective metamaterial [11, 14], or to use numerical computational techniques. The effective

media approach introduced in [11] is employed to design the MIM structure for the 10 µm wavelength in the LWIR spectrum. This specific wavelength is chosen for the prototype as it is the wavelength of maximum emission by the human body. The structure is simulated using the finite-element method (FEM) using COMSOL Multiphysics. Simulated reflection, transmission, and absorption values are obtained by applying an electromagnetic excitation in the space above the structure, then comparing the power incident upon and exiting from the unit cell. A two-dimensional model is employed with Floquet periodicity enforced on the extreme boundaries of the cell orthogonal to the horizontal axis; comparison with a three-dimensional model is used to verify the accuracy of the two-dimensional simulation. Material values for the gold (Au) and silicon dioxide (SiO_2) layers are taken from the literature [15]. The simulations verified that the MIM structure would achieve selective confinement and absorption of electromagnetic energy at the 10 µm wavelength (Fig. 1). The optimum dimensions of the resulting MIM stack are given in Table I.

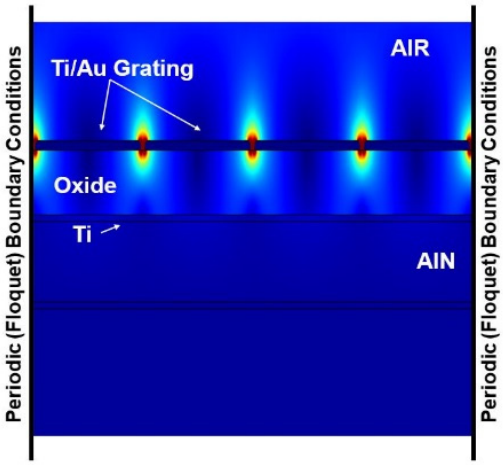

Fig. 1: Electromagnetic simulation (2-D) of the MIM absorber, showing the normalized electric field distribution in the structure when illuminated with IR radiation at a wavelength of 10 µm. The surface plasmon resonance efficiently confines and absorbs the incident radiation, subsequently heating the MIM stack and the underlying substrate (in this case a resonant IR detector).

Table I
MIM Structure and Dimensions

MIM Stack Thickness		
Layer	**Material**	**Thickness**
Bottom Metal (reflector)	Ti	25 nm
Insulator	SiO_2	200 nm
Top Metal (grating)	Ti / Au	5 nm / 30 nm
Grating Dimensions		
Strip Width		750 nm
Gap		100 nm
Pitch		850 nm

III. Integrated Fabrication

The MIM absorber structures were integrated on the top surface of a resonant IR detector, which should be optimized for high thermal isolation and low noise. The fabrication process thus includes steps for both the resonator and the MIM absorber. We use a silicon (Si) wafer as the starting substrate. A 50 nm layer of Pt is deposited and patterned on Si to act as the seed metal layer for AlN deposition. Next, a 500 nm thick layer of AlN is deposited using reactive sputtering. The AlN layer is patterned using a plasma etch, and thin (25 nm) titanium (Ti) electrodes are used as the top electrodes. Thicker Ti/Au layers are deposited for routing and contact pads. The top Ti electrode for the resonator also acts as the bottom metal layer of the MIM stack. The insulator is a thin layer of SiO_2 deposited at 200 °C using low-temperature plasma-enhanced chemical vapor deposition (PECVD). Electron-beam lithography with poly-methyl-methacrylate (PMMA) photoresist is used to pattern a liftoff mask for the top metal grating. The metal lines in the grating consisted of a 5 nm/ 30 nm stack of Ti/Au. The liftoff procedure is carried out in acetone, with careful agitation and ultrasonication.

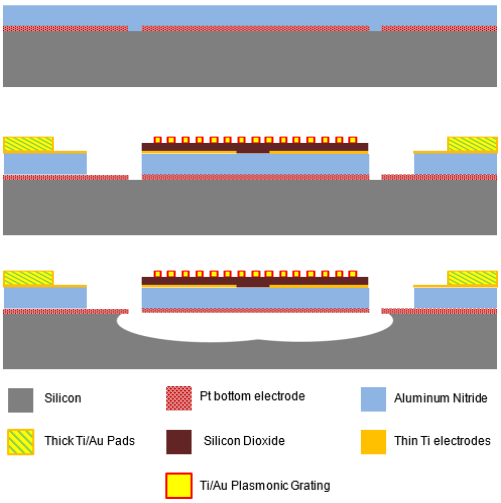

Fig. 2: The fabrication process flow for an AlN based resonant IR detector with an integrated spectrally selective plasmonic IR absorber.

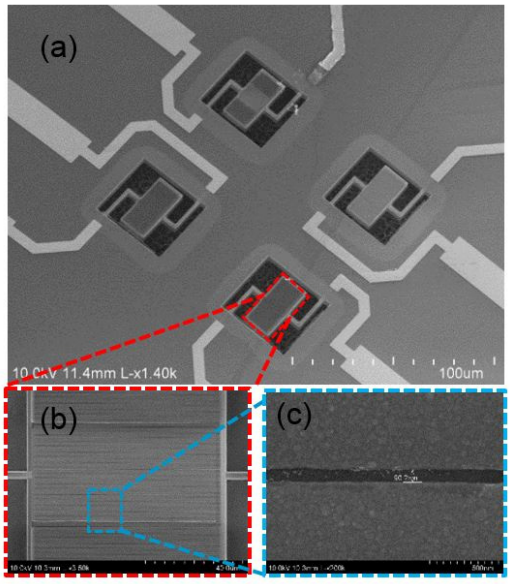

Fig. 3: (a) SEM image of an array of resonant IR detectors (30 µm × 14 µm with 26 µm long crableg tethers). (b) & (c) Magnified SEM images showing the well-defined plasmonic grating with 750 nm wide strips and fabricated gap of 90 nm (design value is 100 nm).

IV. Measured Results

A. MIM Characterization

Characterization of the MIM structures is performed with reflectance spectroscopy using the Perkin-Elmer Spectrum GX Fourier transform infrared (FTIR) spectrophotometer with a KRS-5 gold wire-grid polarizer attachment (Fig. 4). Calibration of the tool for reflectance measurements is accomplished using an Au mirror standard, and calibration for transmittance measurements is performed using air. Reflection $R(\lambda)$ and transmission $T(\lambda)$ measurements are acquired and absorption is inferred from the measurement data using the relation $A(\lambda) = 1 - R(\lambda) - \mathrm{T}(\lambda)$. The experimental absorption measurements match the expected behavior, with a sharp peak at 10.15 μm, with 46% maximum absorption at this wavelength (Fig. 5).

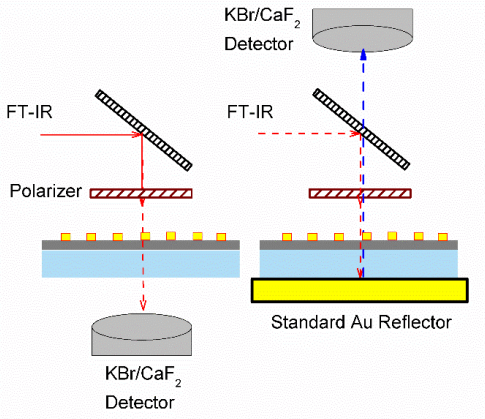

Fig. 4: Measurement setup for IR characterization of the plasmonic absorber gratings. Reflection and Transmission are measured directly, and absorption is inferred. The effect of the substrate and of the background is eliminated using standard calibration procedures. A KRS-5 gold wire-grid polarizer is used to change the polarization angle.

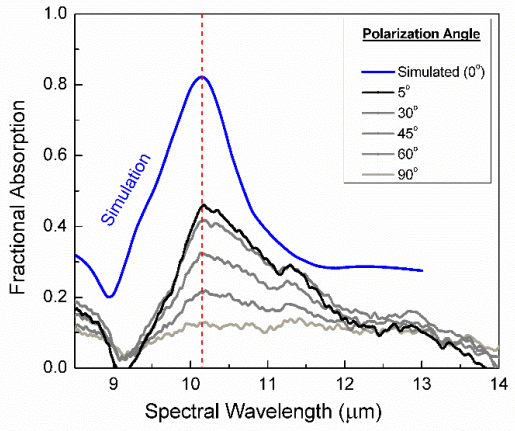

Fig. 5: Measured results of the MIM grating showing a sharp peak at 10.15 μm with a maximum absorption of 46 %. The FWHM of the peak is 1.7 μm, indicating an absorption Q of 6. The absorption is polarization angle dependent. The simulated maximum absorption is > 80%.

The measured results in Fig. 5 are also seen to be polarization angle dependent due to the highly anisotropic nature of the linear gratings. The peak absorption is seen when the magnetic field vector is parallel to the strips and the electric field vector is orthogonal to the strips. A polarization-independent configuration may be developed by replacing the metal strips with structures that are more symmetric, such as metal square patches with the proper dimensions (Fig. 6).

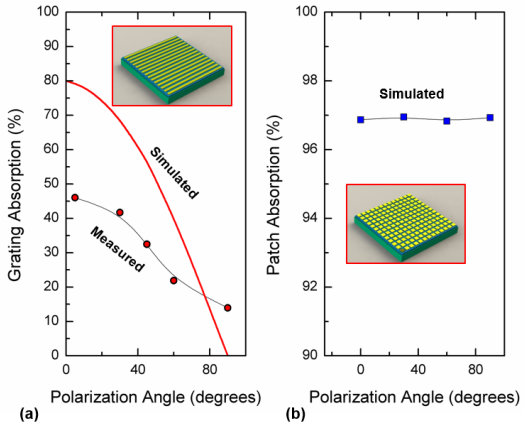

Fig. 6: (a) Measured and simulated results of the MIM grating as a function of the polarization angle. It can be seen that the absorption is strongest when the electric field component is polarized orthogonal to the grating strips. (b) Simulated results show that this polarization dependence can be eliminated by using a polarization insensitive design, such as a square patch pattern MIM structure.

B. Measurement of the Detector Response

The design principles of the resonator itself have been discussed in prior work [6]. The resonators used here are length-extensional mode resonators with AlN as the primary structural material. The AlN plate is 30 μm × 14 μm in size, with two 26 μm long thermally isolating crableg tethers with a thermal conductance (G_{th}) of 3.7×10^{-5} W/K. The heat capacity of the device is 760 pJ/K, leading to a calculated thermal time constant of 20 μs, and a calculated noise equivalent power (NEP) of 362 pW/$\sqrt{\mathrm{Hz}}$ due to thermal fluctuation noise [1, 16], assuming a conservative value of frequency instability of 10^{-10}[6]. Even with the small size, non-conventional tethers and mass loading due to the plasmonic absorbers, the resonators show high performance, operating at 172 MHz with a Q of 1120 at atmospheric pressure and room temperature (Fig. 7).

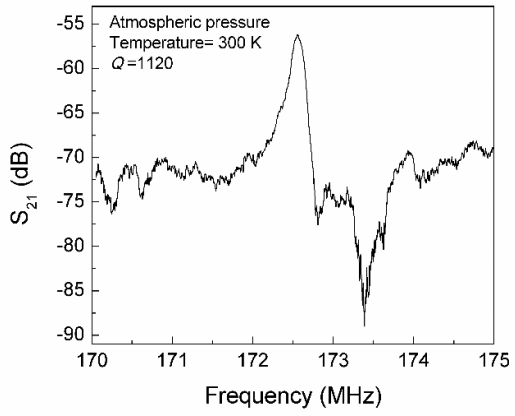

Fig. 7: RF transmission response of an AlN resonator shown with a plasmonic absorber, demonstrating a high mechanical quality factor in spite of the small resonator size, the non-conventional crableg tethers, and the mass loading due to the MIM structure.

When the detectors are illuminated with a broadband thermal radiation source, a frequency shift of ~5.9 kHz can be seen in the peak frequency (Fig. 8). Based on the measured temperature coefficient of frequency (TCF) of -24.3 ppm/K for these devices, we can calculate the temperature rise in the devices to be 1.4 K. Given the thermal isolation provided by the tethers (G_{th} = 3.7×10^{-5} W/K), the absorbed power can be estimated to be 53 µW in the LWIR spectral band centered around 10.15 µm.

A more accurate calibration shall be performed using blackbody sources with traceable calibration for further measurements. The sensitivity of the resonant IR detectors can be improved by an optimized design with a high TCF, or the use of materials, such as GaN, that have a stronger frequency dependence on temperature [4, 5].

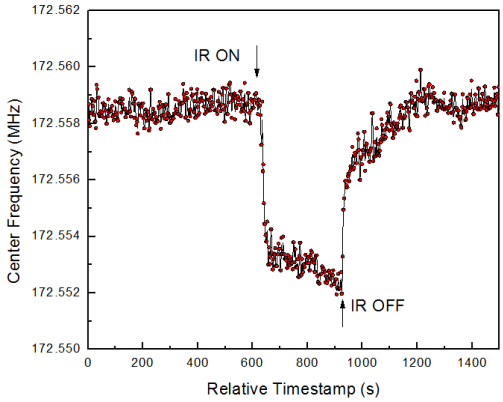

Fig. 8: The sharp shift in the frequency response due to an absorbed power of 53 µW when illuminated by a broadband infrared radiation source.

V. Discussion

This work demonstrated the first instance of a plasmonic grating used as a spectrally selective infrared absorber tuned to a specific wavelength and designed specifically to be integrated with a small, sensitive, and low-noise resonant IR detector. The integrated detector has been implemented and validated. These results can be improved further by optimizing the MIM structure and the resonator design. Based on our simulated results, it is possible to tune the spectral wavelength solely by changing the width and spacing of the top metal grating lines. The spectral tuning range extends from the near-IR to the LWIR (700 nm to 14 µm). This technology can be used for multispectral imaging as well as IR spectroscopy by enabling the implementation of an array of identical resonant detectors with absorbers designed for different wavelengths of IR energy. Further work on the plasmonic absorbers is aimed at (i) improving the sharpness (Q) and magnitude of the absorption peak, (ii) implementing polarization insensitive absorbers, and (iii) improving the tuning range of the absorber peaks.

Acknowledgment

The authors would like to acknowledge Dr. Vishva Ray of the Lurie Nanofabrication Facility (LNF) for assistance with the electron-beam lithography, and Mr. James Windak from the Chemistry Department Technical Services Laboratory for help with FTIR spectroscopic measurements.

References

[1] J. R. Vig, R. L. Filler, and Y. Kim, "Microresonator sensor arrays," *Proc. IEEE Frequency Control Symposium,* pp. 852-869, 1995.

[2] P. Kao and S. Tadigadapa, "Micromachined quartz resonator based infrared detector array," *Sensors and Actuators A: Physical,* vol. 149, pp. 189-192, 2009.

[3] Y. Kim and J. R. Vig, "Experimental results on a quartz microresonator IR sensor," *1997 Ieee Ultrasonics Symposium Proceedings, Vols 1 & 2,* pp. 449-453, 1997.

[4] V. J. Gokhale and M. Rais-Zadeh, "Sensitive uncooled IR detectors using gallium nitride resonators and silicon nitride absorbers," presented at the Solid-State Sensors, Actuators and Microsystems Workshop, Hilton Head, SC, 2012.

[5] V. J. Gokhale, Y. Sui, and M. Rais-Zadeh, "Novel uncooled detector based on gallium nitride micromechanical resonators," *Infrared Technology and Applications Xxxviii, Pts 1 and 2,* vol. 8353, p. 835319, 2012.

[6] V. J. Gokhale and M. Rais-Zadeh, "Uncooled Infrared Detectors Using Gallium Nitride on Silicon Micromechanical Resonators," *Microelectromechanical Systems, Journal of,* vol. accepted Dec 2013, in press, 2013.

[7] Y. Hui, Z. Qian, G. Hummel, and M. Rinaldi, "Pico-watts range uncooled infrared detector based on a freestanding piezoelectric resonant microplate with nanoscale metal anchors," presented at the Solid-State Sensors, Actuators and Microsystems Workshop, Hilton Head Island, South Carolina, 2014.

[8] V. J. Gokhale, O. A. Shenderova, G. E. McGuire, and M. Rais-Zadeh, "Infrared Absorption Properties of Carbon Nanotube/Nanodiamond Based Thin Film Coatings," *Microelectromechanical Systems, Journal of,* vol. 23, pp. 191-197, 2014.

[9] P. Christensen, B. Jakosky, H. Kieffer, M. Malin, H. McSween, Jr., K. Nealson*, et al.*, "The Thermal Emission Imaging System (THEMIS) for the Mars 2001 Odyssey Mission," *Space Science Reviews,* vol. 110, pp. 85-130, 2004/01/01 2004.

[10] C. Wu, B. Neuner, G. Shvets, J. John, A. Milder, B. Zollars*, et al.*, "Large-area wide-angle spectrally selective plasmonic absorber," *Physical Review B,* vol. 84, p. 075102, 08/01/ 2011.

[11] C. Koechlin, P. Bouchon, F. Pardo, J.-L. Pelouard, and R. Haïdar, "Analytical description of subwavelength plasmonic MIM resonators and of their combination," *Optics express,* vol. 21, pp. 7025-7032, 2013.

[12] R. Gordon, "Light in a subwavelength slit in a metal: Propagation and reflection," *Physical Review B,* vol. 73, p. 153405, 2006.

[13] J. Jung, T. Søndergaard, and S. I. Bozhevolnyi, "Gap plasmon-polariton nanoresonators: Scattering enhancement and launching of surface plasmon polaritons," *Physical Review B,* vol. 79, p. 035401, 2009.

[14] J.-T. Shen, P. B. Catrysse, and S. Fan, "Mechanism for designing metallic metamaterials with a high index of refraction," *Physical review letters,* vol. 94, p. 197401, 2005.

[15] E. D. Palik, *Handbook of optical constants of solids* vol. 3: Academic press, 1998.

[16] P. W. Kruse, *Uncooled Thermal Imaging*. Bellingham, WA: SPIE, 2001.